Preprint of paper published as J. Appl. Phys. 110, 043540 (2011)

Enhancement of irradiation-induced defect production in Si nanowires

S. Hoilijoki,[a] E. Holmström, and K. Nordlund
Department of Physics and Helsinki Institute of Physics, University of Helsinki, P.O. Box 64, Helsinki FIN 00014, Finland

(Dated: 24 June 2011)

We performed classical molecular dynamics simulations of defect production in small-diameter hexagonal Si nanowires under Ar ion irradiation. Using irradiation energies of 30 eV to 10 keV, we find that for low energies the defect production in the nanowires may be enhanced by as much as a factor of 3 in comparison to bulk Si due to the large surface-to-volume ratio of the systems. Conversely, at higher energies the increased transmission of ions causes a significant decrease in defect production.

I. INTRODUCTION

Semiconductor nanowires (NW) are seen as a promising class of structures for future nanotechnological applications[1]. Potential industrial applications which have already been demonstrated include field-effect transistors[2,3], sensors for chemical and biological applications[4,5], components in battery technology[6,7], and photonic devices[8–10]. Within the context of semiconductor nanowires, Si is the material which attracts the most attention, owing to the abundance of the material as well as the extensive amount of experience and scientific knowledge on Si accumulated over the previous decades.

In recent years, it has become apparent that electron and ion irradiation may be used to beneficially tailor the properties of many kinds of nanostructures, and hence understanding irradiation effects in nanosystems has become of great and growing interest[11]. Although there is a fair amount of published experimental research on the manufacturing and modification of NWs using ion[12–15] and electron[16–19] irradiation, the amount of results on NWs is currently dwarfed by the body of results on carbon nanotubes[11]. In particular, theoretical studies on the radiation response of NWs are extremely sparse[20,21], in comparison to not just carbon nanotubes, but also such systems as free-standing nanoclusters[22–25]. These observations stand in stark contrast to the fact that ion implantation is the standard method of doping semiconductor components in the industry, and that additionally many prospective applications of NWs are planned for use in high-radiation environments such as space. In this paper, we use classical molecular dynamics (MD) simulations to examine ion irradiation effects in small-diameter hexagonal Si NWs. The aim is to see whether nanoscale effects play a significant role in the defect production of these systems and cause it to deviate from that of bulk Si.

[a] Electronic mail: sanni.hoilijoki@helsinki.fi

II. METHOD

The simulations were performed using classical MD as implemented in the PARCAS code[26]. For modeling the Si–Si interactions, the analytical Stillinger-Weber three-body potential was used[27]. The reason for choosing this potential is that it has been shown to give values for the threshold displacement energies of bulk Si which are, out of the most commonly used empirical potentials for Si, closest to experiment and *ab initio* calculations[28,29]. For the Ar–Si interactions, a purely repulsive ZBL potential[30] was used, as the Coulombic interaction between the two nuclei is the overwhelmingly dominating effect in high-energy collisions. Similary for Si–Si collisions, a repulsive ZBL pair potential was fitted to the high-energy part of the Si–Si interactions, as is the standard practice in the field[31,32]. Additionally, a velocity-dependent electronic stopping power was included in the simulations for all atoms with kinetic energy surpassing 10 eV.

NWs of two different sizes were studied, the larger one having a diameter of $\sim$ 4 nm and comprising 8338 atoms and the smaller one with a diameter of $\sim$ 3 nm and comprising 5000 atoms. Both of the wires were $\sim$ 10 nm Å in length and shared the diamond crystal structure of bulk Si. The axis of the NWs coincided with the $\langle 111 \rangle$ direction, and the wires had a hexagonal cross section with each face of the wire displaying the [112] surface. The 2 x 7.68 surface reconstruction as predicted by experiment[33] and ab initio calculations[34] was taken into account. The motivation for studying this type of NW is that is has been shown to be the most stable small-diameter Si NW[35]. To relax the structures, the wires were annealed slowly from a temperature of 10 to 0 K. Visualizations of the prepared systems are presented in Fig. 1.

To mimic a wire of infinite length, periodic boundary conditions were applied along the longitudal axis of each NW, with 3 Å thick layers fixed at both ends of the wire to prevent the entire system from moving during irradiation. All simulations were done at an initial temperature of 0 K. To model heat dissipation from the impact region into the rest of the NW, Berendsen temperature scaling[36] towards 0 K with a time constant of $\tau = 300$ fs was applied at the periodic boundaries within a layer of thickness of 5 Å.

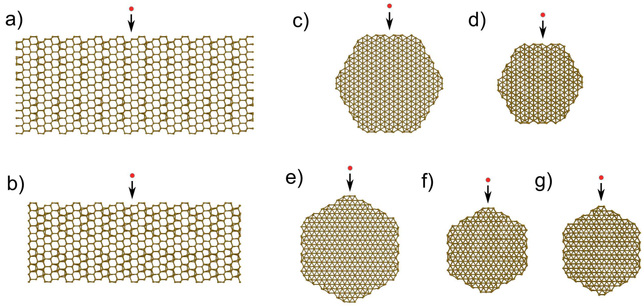

FIG. 1. Visualizations of the studied NWs. a) Sideview of the larger wire of 4 nm diameter showing schematically an incident ion. b) The same for the smaller wire of 3 nm diameter. c) Cross section of the 4 nm wire showing schematically an ion incident on the flat surface. d) The same for the 3 nm wire. e) Cross section of the 4 nm wire showing an ion incident on the edge. f) Cross section of the 3 nm wire showing an ion incident on the first of the two inequivalent edges (“edge 1”). g) Cross section of the smaller wire showing schematically an ion incident on the second of the two inequivalent edges (“edge 2”).

The irradiation runs were organized as follows. Both NWs were irradiated perpendicularly against a flat surface and the edge of the wire. The smaller wire had two inequivalent edge reconstructions, and hence it was irradiated on both of these edges. These different irradiation configurations are schematically visualized in Fig. 1. For each configuration, 200 impact points were chosen randomly uniformly within one repetitive unit cell of the structure, in two dimensions on the flat surface and in one dimension along the edge. Starting from the same initial pristine structure of the wire, each irradiation simulation was run for 20 ps, after which negligible change in the structure was found to take place. Ion energies of 30, 300, 1 000, 3 000, and 10 000 eV were used for all cases. Additionally, for comparing the results of the NW simulations with the behavior of bulk Si, self-recoils in bulk Si as well as Ar ion irradiation of a reconstructed [001] Si slab surface were simulated using an analogous simulation setup. The simulated slab was chosen to be large enough so that no transmission of ions occurred at the studied energies.

After the irradiation runs, Voronoy polyhedron analysis[37] was performed for analyzing defects in the end states of the irradiated systems. Using this method, vacancies and interstitials were identified in the structures. Additionally, adatoms and sputtered atoms were analyzed for by considering any atom at a distance of 1 to 3 Å from the wire surface an adatom and any atom further than 3 Å from the surface to be sputtered.

Finally, to gain further insight into the MD results, binary collision approximation[38] (BCA) simulations of irradiation of sheets of Si with Ar ions were carried out using the SRIM package[38,39]. In these runs, the threshold displacement energy of Si in the BCA simulation was first normalized to the value of 24 eV to give the same amount of vacancies per incident ion as the larger simulated NW with an ion energy of 1 keV. The SRIM simulations were then run for two sheets of Si with thicknesses corresponding to the effective diameters of the two nanowires, with energies in the same range as in the MD runs.

III. RESULTS AND DISCUSSION

A typical example of the end state of the 4 nm wire after an irradiation run is presented for each ion energy in Fig. 2[40]. For 30 eV, the ion deposits its energy within the first couple of atomic layers, and the damage is confined to the surface. At 300 eV, a small collision cascade is formed at the surface, and the ion penetrates a distance of $\sim$ 1 nm into the wire. Beyond this energy, the ion is very likely to traverse the entire cross section of the wire. At 1000 eV, the ion is deflected in the core and exits through one of the surfaces in the lower half of the wire, creating small cascades upon entering and exiting the wire. At 3000 eV, the cascades are larger. Finally at 10 000 eV, transmission of the ion with often little energy deposited in the system becomes a common case. The damage is mainly formed upon entering and exiting the wire, again.

This general conclusion of the damage being predominantly created on the surfaces of the wire is confirmed by the distribution of the positions of the vacancies and interstitials created in the wires by the irradiation. In Fig. 5, the ratio of the density of defects produced at 1 keV to the density of atoms in the pristine wire, C_{def}, is presented as a function of perpendicular distance from the surface of each wire. The same analysis is also presented for a thick Si slab. From the Figure, it can be seen that defect production in the wires is concentrated in the couple of outermost atomic layers of the structures, whereas for the slab the distribution is comparatively flat with only a slight increase towards the surface. As regards the separate distributions of vacancies and interstitials, the respective distributions are plotted for the 3 nm wire after 1 keV irradiation of the flat surface in Fig. 6. It can be seen here that vacancies and interstitials are created in equal amounts in the core of the wire, but vacancies dominate on the surface. This is because sputtered atoms leave a vacancy but no interstitial in the wire.

The above results can be explained by considering the threshold energy for sputtering on the surface and the threshold energy for displacement in the core of the wire, along with the range of ions in Si. Firstly, defect production is highest on the surface of the wire because the threshold energy for damage production on the surface can be smaller than the threshold energy for displacement in the core of the wire by a factor of 2 to 3[21]. Secondly, as the energy of the incoming ion increases, the range of the ion shifts from the top surface of the wire towards the bottom surface and beyond, explaining the positions of the created cascades. At 10 000 eV, the ion range is already large enough that transmission of the ion with

little energy deposited in the wire is the dominating outcome of the irradiation events.

The surface reconstruction of the wire is generally preserved well after an ion impact. For e.g. 1 keV irradiation of the 4 nm wire, roughly 40% of all cases are such that the surface remains intact after the impact event. When the surface does get modified, the damage to the surface reconstruction is typically on the range of a couple of unit cells in both horizontal directions in the plane of the surface, never extending further than a few unit cells. The damage is likewise confined to local spots on the surface where the ion exits the wire. Examples of damage to the first two atomic layers on the surface of the wire where the ion enters and the bottom of the wire in cases where the ion exits there are shown in Fig. 3.

Results for the total number of defects for the flat surface of each NW and the bulk and slab are presented as a function of ion energy in Fig. 4. While the defect production in bulk Si increases almost linearly with increasing ion energy, the behavior of the NWs and the slab is more interesting. There is a clear enhancement of defect production for the smaller wire of 3 nm diameter at 1 keV, approximately by a factor of 3 as compared to bulk and slab Si, and a similar but less significant enhancement for the larger wire of 4 nm diameter as well. For high energies, defect production decreases for both of the NWs, whereas for the slab the rate of increase drops as ion energy increases. Since the defect production was shown above to take place predominantly on the surfaces of the wires, at a suitable ion range we would indeed expect enhancement in the defect production in the wires in comparison to bulk Si or a thick Si slab. Such a range is given here at 1 keV for both wires. The enhancement in comparison to bulk Si is greater for the smaller 3 nm wire, because there the surface-to-volume ratio is greater than in the 4 nm wire. This finite-size effect is demonstrated clearly in Fig. 5, where it is seen that the larger the surface-to-volume ratio of the system, the stronger the increase in defect concentration towards the surface.

As regards the observed decrease in defect production in the NWs for high ion energies, we refer to the results of the SRIM calculations for the larger wire as presented in Fig. 7. We see that these BCA results for the number of produced vacancies follow the MD results very closely, and thus the decrease in defect production in the wire at high ion energies can be attributed to the increased transmission of ions for increasing irradiation energy, an effect which is well understood in irradiation of thin specimens[30]. In the initially crystalline wires, this effect is coupled with the additional effect of channeling which then causes the vacancy production in the MD runs to decrease at a faster rate than the SRIM results for high energies.

Finally, the results for the total number of defects for all the NW irradiations are presented in Fig. 8. It can be seen that defect production varies clearly between the NW size and whether the flat surface or the edge was considered. The differences between the flat surface and the edges are most likely due to stronger channeling for ions incident on the edges of the wires. As concluded above, defect production in the wires is mainly a surface effect, and indeed the small wire has the most radiation damage in general.

IV. CONCLUSIONS

In conclusion, ion irradiation of small-diameter Si NWs was studied using classical MD. It was found that defect production in the systems is largely a surface effect, leading to an enhancement of up to a factor of three as compared to bulk Si, due to the large surface-to-volume ratio of the NWs. For high irradiation energies, the increased transmission of ions coupled with the channeling effect causes a notable decrease in defect production in the wires.

ACKNOWLEDGMENTS

This work was supported by the Academy of Finland Centre of Excellence in Computational Molecular Science. Generous grants of computer time from the Center for Scientific Computing in Espoo, Finland are gratefully acknowledged.

[1] W. Lu and C. M. Lieber, J. Phys. D: Appl. Phys. **39**, R387 (2006).
[2] Y. Cui, Z. Zhong, D. Wang, W. U. Wang, and C. M. Lieber, Nano Lett. **3**, 149 (2003).
[3] J. Goldberger, A. I. Hochbaum, R. Fan, and P. Yang, Nano Lett. **6**, 973 (2006).
[4] Y. Cui, Q. Wei, H. Park, and C. M. Lieber, Science **293**, 1289 (2001).
[5] G. Zheng, F. Patolsky, Y. Cui, W. U. Wang, and C. M. Lieber, Nature Biotech. **23**, 1294 (2005).
[6] C. K. Chan, H. Peng, G. Liu, K. McIlwrath, X. F. Zhang, R. A. Huggins, and Y. Cui, Nature Nanotech. Lett. **3**, 31 (2008).
[7] L. Cui, R. Ruffo, C. K. Chan, H. Peng, and Y. Cui, Nano Lett. **9**, 491 (2008).
[8] M. S. Gudiksen, L. J. Lauhon, J. Wang, D. C. Smith, and C. M. Lieber, Nature **415**, 617 (2002).
[9] C. J. Barrelet, A. B. Greytak, and C. M. Lieber, Nano Lett. **4**, 1981 (2004).
[10] C. J. Barrelet, J. Bao, M. Loncar, H.-G. Park, F. Capasso, and C. M. Lieber, Nano Lett. **6**, 11 (2006).
[11] A. V. Krasheninnikov and K. Nordlund, J. Appl. Phys. (Applied Physics Reviews) **107**, 071301 (2010).
[12] J. Chen and R. Könenkamp, Appl. Phys. Lett. **82**, 4782 (2003).
[13] S. Dhara, A. Datta, C. T. Wu, Z. H. Lan, K. H. Chen, Y. L. Wang, C. W. Hsu, C. H. Shen, L. C. Chen, and C. C. Chen, Appl. Phys. Lett. **84**, 5473 (2004).
[14] A. Colli, A. Fasoli, C. Ronning, S. Pisana, S. Piscanec, and A. C. Ferrari, Nano Lett. **8**, 2188 (2008).
[15] S. Hoffmann, J. Bauer, C. Ronning, T. Stelzner, J. Michler, C. Ballif, V. Sivakov, and S. H. Christiansen, Nano Lett. **9**, 1341 (2009).
[16] Y. Kondo and K. Takayanagi, Phys. Rev. Lett. **79**, 3455 (1997).
[17] S. Xu, M. Tian, J. Wang, J. Xu, J. M. Redwing, and M. H. W. Chan, Small **1**, 1221 (2005).
[18] T. Aref, M. Remeika, and A. Bezryadin, J. Appl. Phys. **104**, 024312 (2008).

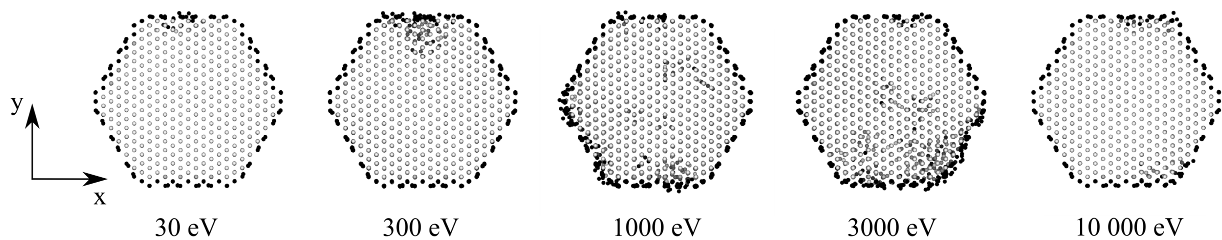

FIG. 2. An example of the end state of an irradiation run for each of the used irradiation energies for the 4 nm wire. The ion is incident on the top surface. The coloring is by potential energy, with dark being high.

FIG. 3. Examples of damage to the first two atomic layers on the surface of the wire where the ion enters (left) and the bottom of the wire where the ion exits (right). The extent of the damage is usually limited to a couple unit cells in both dimensions. Coloring is by distance from the core of the wire, with dark being closer to the core.

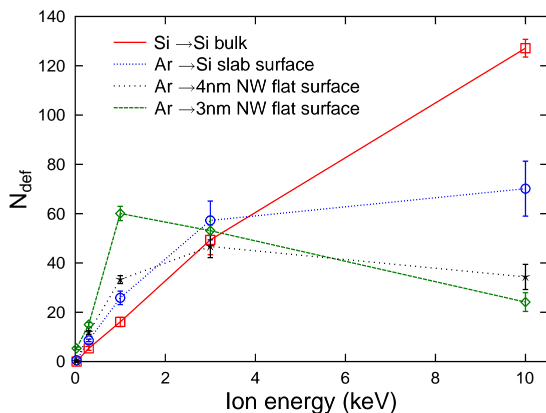

FIG. 4. Results for the total number of defects for the irradiation of bulk Si, a thick Si slab surface, and the flat surfaces of the NWs.

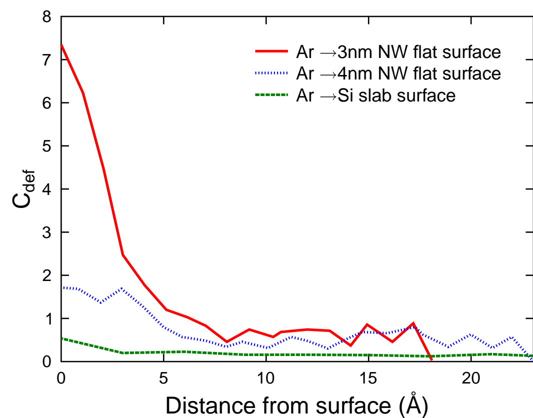

FIG. 5. Concentration (see text) of point defects (vacancies or interstitials) created by 1 keV irradiation during the entire set of runs as a function of distance from the surface of the wires and a thick Si slab surface.

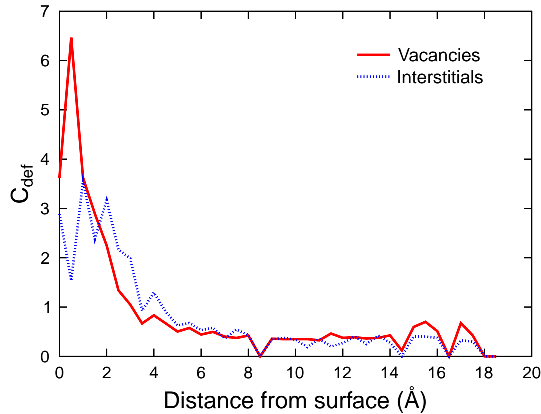

FIG. 6. Separate concentrations (see text) of vacancies and interstitials created by 1 keV irradiation during the entire set of runs for the 3 nm wire as a function of distance from the surface.

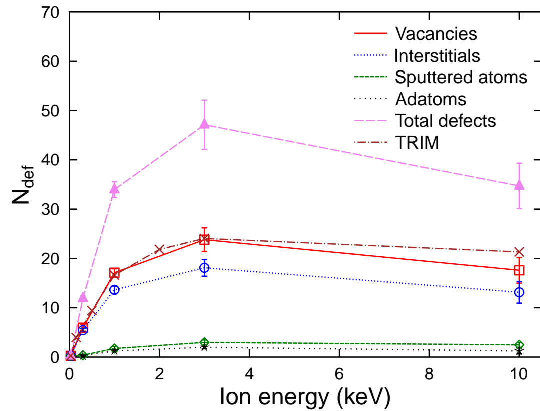

FIG. 7. Results for the total number of each type of defect produced in the MD runs on the 4 nm wire flat surface and results of TRIM simulations on the number of vacancies produced in a sheet of Si with a thickness equal to the effective diameter of the same wire.

[19] J. Hu, Q. Li, J. Zhan, Y. Jiao, Z. Liu, S. P. Ringer, Y. Bando, and D. Golberg, ACS Nano **2**, 107 (2008).
[20] C. S. Moura and L. Amaral, Nucl. Inst. Meth. Res. B **228**, 37 (2005).
[21] E. Holmström, L. Toikka, A. V. Krasheninnikov, and K. Nordlund, Phys. Rev. B. **82**, 045420 (2010).
[22] R. Kissel and H. M. Urbassek, Nucl. Instr. Meth. Phys. Res. B **180**, 293 (2001).
[23] S. Zimmermann and H. M. Urbassek, Int. J. Mass Spectrom. **272**, 91 (2008).
[24] T. T. Järvi, J. A. Pakarinen, A. Kuronen, and K. Nordlund, Europhys. Lett. **82**, 26002 (2008).
[25] T. T. Järvi, D. Pohl, K. Albe, B. Rellinghaus, L. Schultz, J. Fassbender, A. Kuronen, and K. Nordlund, Europhys. Lett. **85**, 26001 (2009).

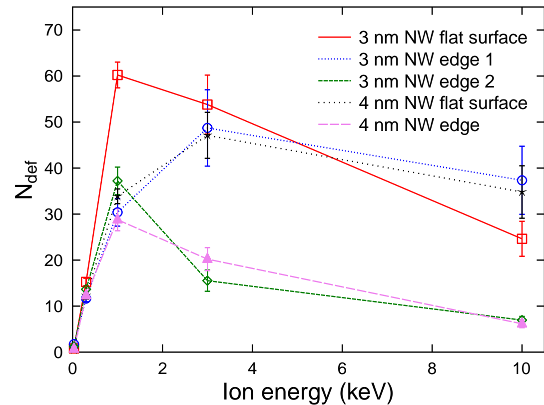

FIG. 8. Results for the total number of defects for all NW irradiation runs.

[26] K. Nordlund(2006), PARCAS computer code. The main principles of the molecular dynamics algorithms are presented in[37,41]. The adaptive time step and electronic stopping algorithms are the same as in[42].
[27] F. H. Stillinger and T. A. Weber, Phys. Rev. B **31**, 5262 (1985).
[28] E. Holmstrom, A. Kuronen, and K. Nordlund, Phys. Rev. B **78**, 045202 (2008).
[29] E. Holmström, A. V. Krasheninnikov, and K. Nordlund, in *Ion Beams and Nano-Engineering*, MRS Symposium Proceedings, edited by D. Ila, J. K. N. Lindner, P. K. Chu, J. Baglin, and N. Kishimoto (MRS, Warrendale, PA, USA, 2009).
[30] J. F. Ziegler, J. P. Biersack, and U. Littmark, *The Stopping and Range of Ions in Matter* (Pergamon, New York, 1985).
[31] T. Aoki, S. Chiba, J. Matsuo, I. Yamada, and J. P. Biersack, Nucl. Inst. Meth. Phys. Res. B **180**, 312 (2001).
[32] T. Aoki, J. Matsuo, and G. Takaoka, Nucl. Inst. Meth. Phys. Res. B **202**, 278 (2003).
[33] C. Fulk, S. Sivananthan, D. Zavitz, R. Singh, M. Trenary, Y. P. Chen, G. Brill, and N. Dhar, J. Electr. Mat. **35**, 1449 (2006).
[34] C. H. Grein, J. Crys. Growth **180**, 54 (1997).
[35] I. Ponomareva, M. Menon, D. Skrivastava, and A. N. Ansdriotis, Phys. Rev. Lett. **95**, 265502 (2005).
[36] H. J. C. Berendsen, J. P. M. Postma, W. F. van Gunsteren, A. DiNola, and J. R. Haak, J. Chem. Phys. **81**, 3684 (1984).
[37] K. Nordlund, M. Ghaly, R. S. Averback, M. Caturla, T. Diaz de la Rubia, and J. Tarus, Phys. Rev. B **57**, 7556 (1998).
[38] J. F. Ziegler, J. P. Biersack, and M. D. Ziegler, *SRIM - The Stopping and Range of Ions in Matter* (SRIM Co., Chester, Maryland, USA, 2008).
[39] J. F. Ziegler, SRIM-2008 software package, available online at *http://www.srim.org*.
[40] A. Stukowski, Modelling Simul. Mater. Sci. Eng. **18**, 015012 (2010).
[41] M. Ghaly, K. Nordlund, and R. S. Averback, Phil. Mag. A **79**, 795 (1999).
[42] K. Nordlund, Comput. Mater. Sci. **3**, 448 (1995).